JPEDAV (2008) 29:477–481
DOI: 10.1007/s11669-008-9390-0
1547-7037 ©ASM International



# Microstructural Evidence of $\beta Co_2Si$-phase Stability in the Co-Si System

*Renato Baldan, Maria Ismênia Sodero Toledo Faria, Carlos Angelo Nunes, Gilberto Carvalho Coelho, Vanessa Motta Chad, and Roberto Ribeiro de Avillez*

*(Submitted March 28, 2008; in revised form June 26, 2008)*

**The aim of this work was to verify the stability of the $\beta Co_2Si$ phase in the Co-Si system. The samples were produced via arc-melting and characterized through Scanning Electron Microscopy (SEM) and Differential Thermal Analysis (DTA). The results have confirmed the stability of the $\beta Co_2Si$ phase, however, a modification of the shape of $\beta Co_2Si$ phase field is proposed in order to fully explain the results.**

**Keywords** $\beta Co_2Si$, Co-Si system, silicides

## 1. Introduction

Co-based alloys can be developed to produce materials with interesting magnetic properties,[1,2] as is the case of Co-Si-B alloys. In this context, information concerning phase stability becomes fundamental for alloy processing and application.

The currently accepted phase diagram of the Co-Si system is shown in Fig. 1.[3] This diagram presents the $Co_2Si$ stoichiometry with two structures: $\alpha Co_2Si$, orthorhombic and stable below 1320 °C and $\beta Co_2Si$, stable between 1238 °C and 1334 °C with non-determined crystal structure. The $\beta Co_2Si$ phase was first proposed by Vogel[4] in the study of the Fe-Co-Si system in the region between 0 and 32.45 wt.% Si. The proposal of $\beta Co_2Si$ was based on the interpretation of thermal analysis curves and optical microscopy images of the resultant microstructures. Although no thermal event could be clearly associated with the transition $\alpha Co_2Si \leftrightarrow \beta Co_2Si$, the observed thermal events in hyperstoichiometric alloys had suggested the existence of the $\beta Co_2Si$ phase. However, the material used for the sample preparation presented iron traces, generating doubts with respect to the existence of a stable $\beta Co_2Si$ phase in the Co-Si system.

In a recent study aiming at the characterization of as-cast Co-Si alloys,[5] no indication of the $\beta Co_2Si$ phase was observed. Thus, in this work a systematic investigation was carried out to verify the possible stability of the $\beta Co_2Si$-phase in the Co-Si system, which was indeed confirmed by the present results.

**Renato Baldan, Maria Ismênia Sodero Toledo Faria, Carlos Angelo Nunes, Gilberto Carvalho Coelho,** and **Vanessa Motta Chad,** Universidade de São Paulo (USP), Escola de Engenharia de Lorena (EEL), Pólo Urbo-Industrial Gleba AI-6, C.P. 116 CEP 12600-970 Lorena, São Paulo, Brazil; **Roberto Ribeiro de Avillez,** Departamento de Ciência dos Materiais e Metalurgia (DCMM), Pontifícia Universidade Católica do Rio de Janeiro (PUC-Rio), Rua Marques de São Vicente, 225, CEP 22453-900 Gavea, Rio de Janeiro, RJ, Brazil. Contact e-mail: renato@ppgem.eel.usp.br.

## 2. Experimental Procedure

The alloy compositions produced in this work were prepared from Co (min. 99.97%) and Si (min. 99.999%). The samples were arc-melted under an argon atmosphere in a water-cooled copper crucible with a non-consumable tungsten electrode. Before the melt of each alloy, a Ti getter was melted to absorb any contaminants that might be present in the argon atmosphere. Each sample was melted four times to guarantee the complete dissolution of the elements and the chemical homogeneity of the alloy. Subsequently, each sample was weighed to evaluate any mass losses that might be associated with the melting steps. The composition intervals for each sample were calculated, attributing all the mass losses to either Co or Si volatilization. The nominal composition for each alloy was taken to be the mean value of this interval.

The as-cast microstructures were evaluated via scanning electron microscope (SEM) operating in the back-scattered electron mode (BSE). For the SEM analysis, the samples were prepared following standard metallographic procedures: hot mounting in resin; grinding in the sequence #320-#2400 SiC sand paper; and polishing with colloidal silica suspension (OP-S). None of the samples were etched. The images were obtained in a LEO 1450VP SEM instrument. Selected samples (~40 mg) were submitted to differential thermal analysis (DTA) in a Perkin Elmer DTA 7 instrument with 20 °C/min heating and cooling rates.

## 3. Results and Discussion

The initial and final sample mass, the respective mass variations due to the melting steps, and the nominal sample compositions are indicated in Table 1.

The solidification of sample 66.17Co33.83Si (Fig. 2a, b) started with the formation of primary crystals of $\beta Co_2Si$,

**Table 1 Target and nominal compositions of the Co-Si alloys, mass losses associated to the melting steps and the calculated composition interval for each sample supposing that all mass losses were either from Co or Si volatilization**

| Target composition, at.% Si | Sample mass | | Mass loss, % | Composition range, at.% Si | Nominal composition, at.% |
|---|---|---|---|---|---|
| | Before melt, g | After melt, g | | | |
| 32 | 4.09720 | 4.08170 | −0.378 | 31.54 to 32.09 | 68.19Co31.81Si |
| 33 | 3.98970 | 3.97570 | −0.351 | 32.57 to 33.08 | 67.17Co32.83Si |
| 34 | 4.08480 | 4.07020 | −0.357 | 33.58 to 34.09 | 66.17Co33.83Si |
| 35 | 4.13130 | 4.11100 | −0.491 | 34.45 to 35.14 | 65.21Co34.79Si |
| 36 | 4.15220 | 4.13740 | −0.356 | 35.62 to 36.11 | 64.13Co35.87Si |
| 37 | 2.99900 | 2.99870 | −0.010 | 37.02 to 37.03 | 62.97Co37.03Si |

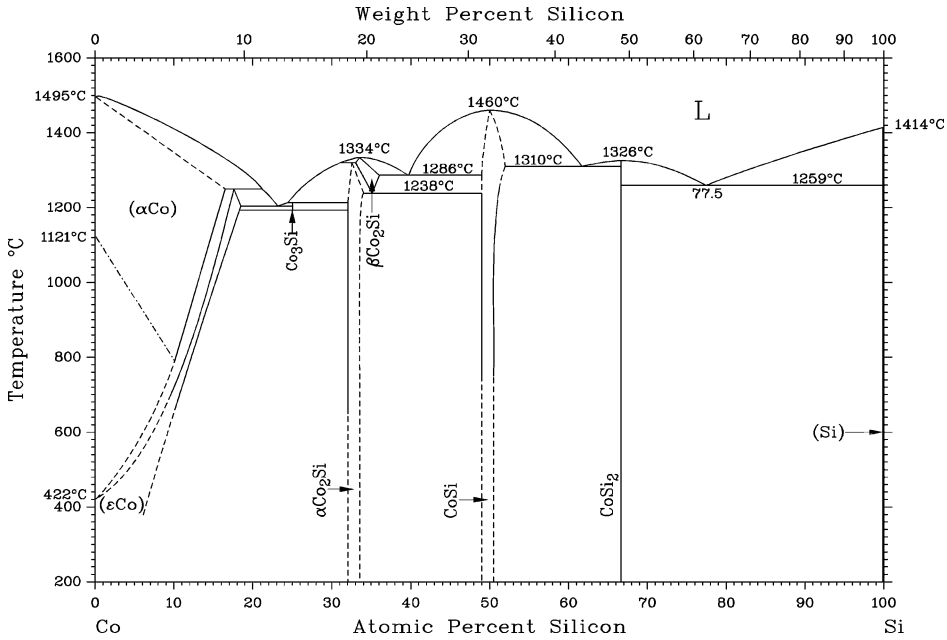


**Fig. 1** Currently accepted Co-Si phase diagram[3]

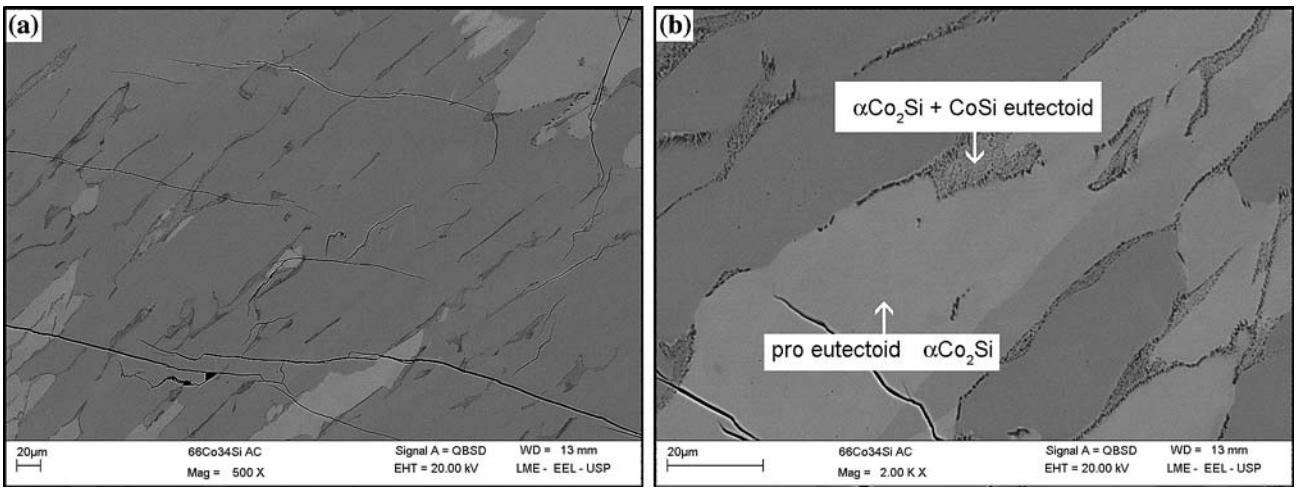


**Fig. 2** SEM-BSE micrographs of as-cast 66.17Co33.83Si (a, b), 65.21Co34.79Si (c, d), 64.13Co35.87Si (e, f) and 62.97Co37.03Si (g, h) alloys

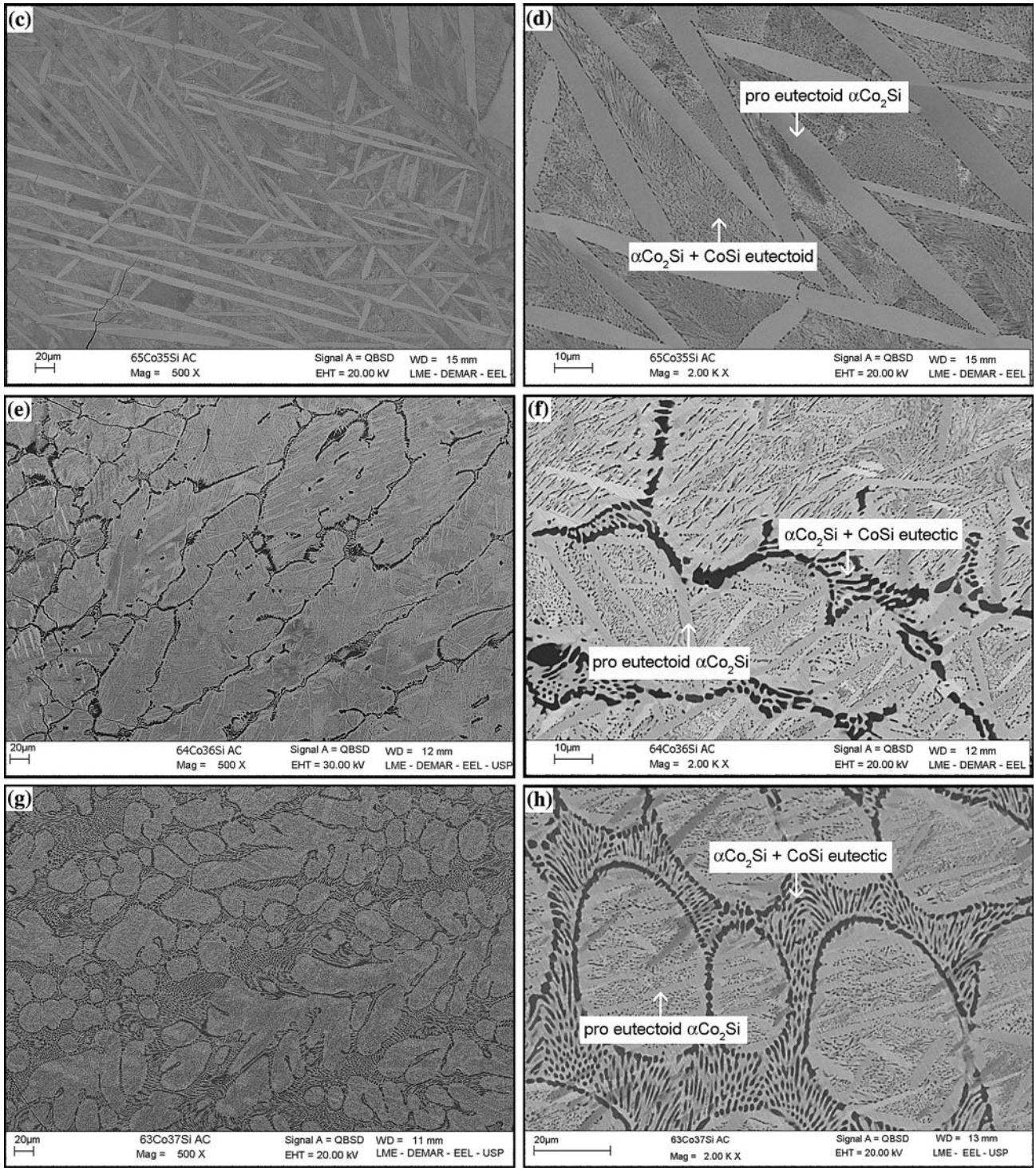


**Fig. 2 (continued)** SEM-BSE micrographs of as-cast 66.17Co33.83Si (a, b), 65.21Co34.79Si (c, d), 64.13Co35.87Si (e, f) and 62.97Co37.03Si (g, h) alloys

which grow across the L + $\beta Co_2Si$ field and the solidification ends with a $\beta Co_2Si$ single-phase microstructure. With further cooling, a gradual formation and growth of $\alpha Co_2Si$ from $\beta Co_2Si$ takes place and, finally, the remaining $\beta Co_2Si$ transforms into $\alpha Co_2Si$ + CoSi through a eutectoid reaction. The large pro-eutectoid volume fraction of $\alpha Co_2Si$ is clearly noticed in the micrographs of this alloy.

The sample 65.21Co34.79Si (Fig. 2c, d) presented the same sequence of phase transformations as the previous sample, however, with smaller volume fraction of plate-like

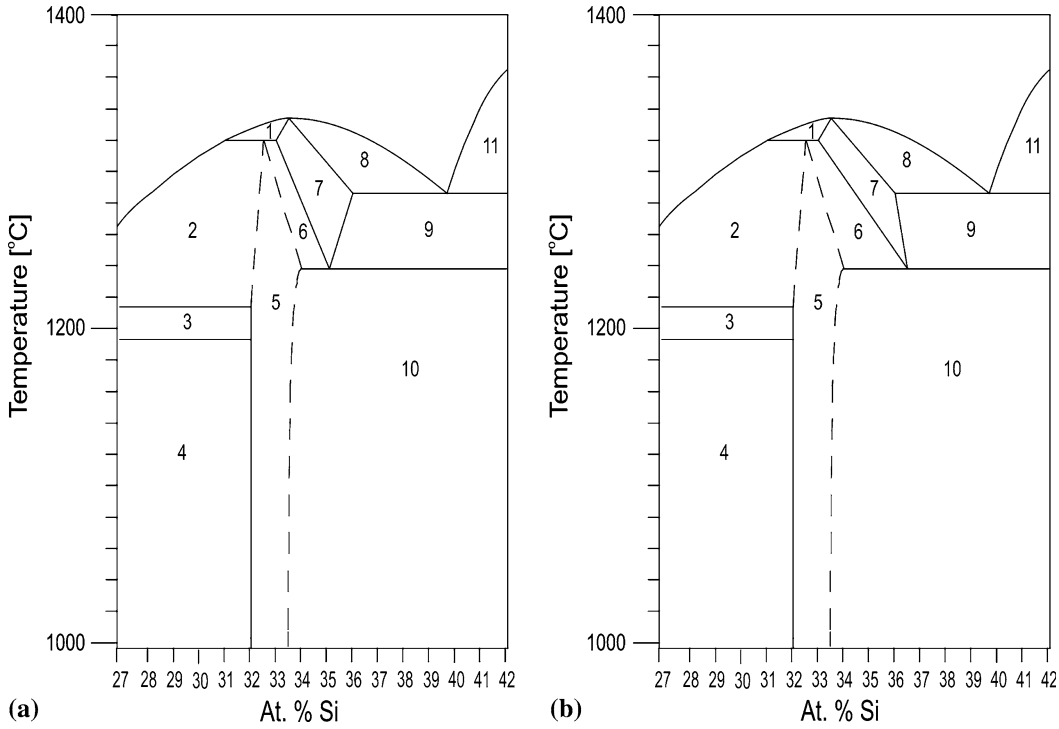


**Fig. 3** Phase diagram of the Co-Si in the region between 27 and 42 at.% Si: (a) Currently accepted diagram; (b) Modified diagram. (1) $\beta Co_2Si$ + L; (2) $\alpha Co_2Si$ + L; (3) $\alpha Co_2Si$ + $Co_3Si$; (4) εCo + $\alpha Co_2Si$; (5) $\alpha Co_2Si$; (6) $\beta Co_2Si$ + $\alpha Co_2Si$; (7) $\beta Co_2Si$; (8) $\beta Co_2Si$ + L; (9) $\beta Co_2Si$ + CoSi; (10) $\alpha Co_2Si$ + CoSi; (11) CoSi + L

pro-eutectoid $\alpha Co_2Si$, and a larger volume fraction of $\alpha Co_2Si$ + CoSi regions associated with the eutectoid $\beta Co_2Si \leftrightarrow \alpha Co_2Si$ + CoSi reaction.

The solidification of sample 64.13Co35.87Si is also initiated with the formation of primary $\beta Co_2Si$ crystals, which grow across the L + $\beta Co_2Si$ field. However, in this case, the final liquid undergoes the invariant L ↔ $\beta Co_2Si$ + CoSi eutectic reaction. Then, pro-eutectoid $\alpha Co_2Si$ forms from $\beta Co_2Si$ during cooling across the $\beta Co_2Si$ + $\alpha Co_2Si$ two-phase field, this is clearly evident in the primary $\beta Co_2Si$ dendrites in Fig. 2(e) and (f). Finally, the remaining $\beta Co_2Si$ undergoes the eutectoid $\beta Co_2Si \leftrightarrow \alpha Co_2Si$ + CoSi reaction.

Sample 62.97Co37.03Si (Fig. 2g, h) presented the same sequence of phase transformation shown by the previous sample, however, with smaller volume fraction of primary phase and, consequently, larger volume fraction of eutectic L ↔ $\beta Co_2Si$ + CoSi regions. Again, evidence of solid state transformations in primary $\beta Co_2Si$ dendrites can be noted.

Pro-eutectoid $\alpha Co_2Si$ plates are observed homogeneously distributed in the $\beta Co_2Si$ primary dendrites in samples 64.13Co35.87Si (Fig. 2e, f) and 62.97Co37.03Si (Fig. 2g, h). An enlargement of the region of interest in the Co-Si phase diagram is shown in Fig. 3(a). According to this figure, the Si content of the $\beta Co_2Si$ phase at the eutectic temperature is larger than that at the eutectoid temperature. Thus, under equilibrium conditions, during cooling from the eutectic to the eutectoid temperature, the $\beta Co_2Si$ + $\alpha Co_2Si$ two-phase field could not be crossed and, in this way, no pro-eutectoid $\alpha Co_2Si$ could have been formed. Cored $\beta Co_2Si$ dendrites with regions presenting Si contents smaller than the equilibrium composition at the eutectoid temperature could also produce pro-eutectoid $\alpha Co_2Si$. However, in this case, the pro-eutectoid formation of $\alpha Co_2Si$ should not be homogeneously distributed as shown in Fig. 2(e)-(h). Thus, a different shape of the $\beta Co_2Si$ field is possible and shown in Fig. 3(b). However, it should be pointed out that, due to the proximity of the eutectic and eutectoid invariant reactions and the reasonably fast cooling rates of these samples, metastable transformations may have lead to those features, and in this case, the $\beta Co_2Si$-phase field present in the currently accepted phase diagram might be correct. It was not the purpose of this work to elucidate completely this matter.

Evidence of the stability of $\beta Co_2Si$ has also been found through DTA experiments of the 66.17Co33.83Si, 65.21Co34.79Si, and 64.13Co35.87Si samples. Figure 4 presents DTA curves of the 64.13Co35.87Si sample, displaying three peaks on heating and two peaks on cooling. During heating, the peak at 1251 °C can be associated with the $\alpha Co_2Si$ + CoSi → $\beta Co_2Si$ reaction, the peak at 1298 °C with the reaction $\beta Co_2Si$ + CoSi → L, and the one at 1326 °C with the melting of the remaining $\beta Co_2Si$ phase. During cooling, the peak at 1294 °C refers to the solidification of the sample, where the thermal effects associated with the primary precipitation of $\beta Co_2Si$ is superimposed with that associated with the L → $\beta Co_2Si$ + CoSi eutectic decomposition. Furthermore, the peak at

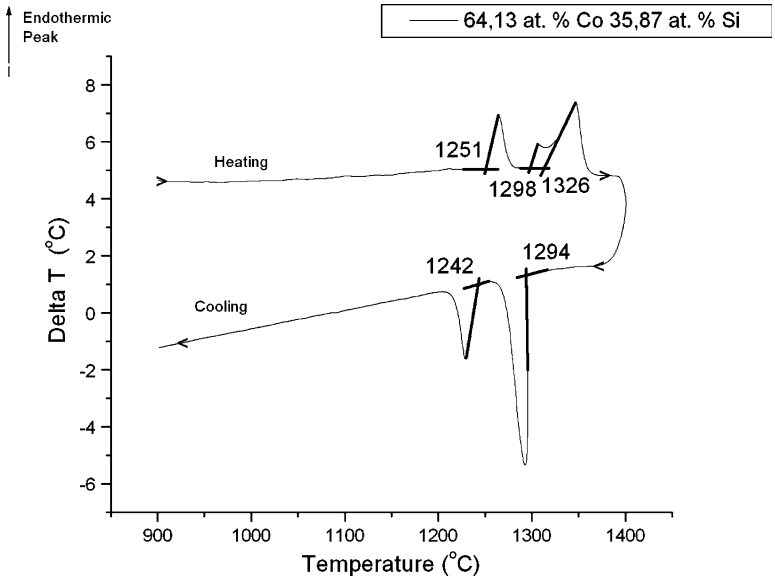


**Fig. 4** Differential thermal analysis curve of 64.13Co35.87Si sample

1242 °C refers to the $\beta Co_2Si \rightarrow \alpha Co_2Si + CoSi$ eutectoid decomposition.

## 4. Conclusions

The stability of the $\beta Co_2Si$-phase in the Co-Si system as well as the eutectoid $\beta Co_2Si \leftrightarrow \alpha Co_2Si + CoSi$ reaction have been confirmed by microstructural (SEM) and differential thermal analysis (DTA) characterization of Co-Si alloys with composition in the 32-37 at.% Si interval. However, a modification in the shape of the $\beta Co_2Si$ phase field is proposed in order to explain the observed pro-eutectoid formation of $\alpha Co_2Si$ in the highest Si contents alloys.

## References

1. I.C. Rho, C.S. Yoon, C.K. Kim, T.Y. Byun, and K.S. Hong, Crystallization of Amorphous Alloy CoFeCrSiB, *Mater. Sci. Eng.*, 2002, **B96**, p 48-52
2. M. Pekala, M. Jachimowicz, V.I. Fadeeva, and H. Matyja, Phase Transformations in Co-B-Si Alloys Induced by High-energy Ball Milling, *J. Non-Cryst. Solids*, 2001, **287**, p 360-365
3. T.B. Massalski, H. Okamoto, P.R. Subramanian, and L. Kacprzak, *Binary Alloy Phase Diagrams*, 2nd ed., Vol. 2, ASM, Materials Park, OH, 1990, p 1235-1239
4. R. Vogel and K. Rosenthal, Das Zustandsschaubild Kobalt-Silizium, *Arch. für das Eisenhüttenwesen*, 1934, **12**, p 689-691, in German
5. M.I.S.T. Faria, G.C. Coelho, C.A. Nunes, and R.R. Avillez, Microstructural Characterization of as Cast Co-Si Alloys, *Mater. Charact.*, 2006, **56**, p 66-72